Preparation for quantum simulation of the (1 + 1)-dimensional O(3) nonlinear σ model using cold atoms

Anthony N. Ciavarella,[*] Stephan Caspar,[†] Hersh Singh,[‡] and Martin J. Savage[§]
InQubator for Quantum Simulation (IQuS), Department of Physics, University of Washington, Seattle, Washington 98195-1550, USA

(Received 25 November 2022; accepted 21 March 2023; published 4 April 2023)

The (1+1)-dimensional (1+1D) O(3) nonlinear σ-model is a model system for future quantum lattice simulations of other asymptotically free theories, such as non-Abelian gauge theories. We find that utilizing dimensional reduction can make efficient use of two-dimensional layouts presently available on cold-atom quantum simulators. A different definition of the renormalized coupling is introduced, which is applicable to systems with open boundary conditions and can be measured using analog quantum simulators. Monte Carlo and tensor network calculations are performed to determine the quantum resources required to reproduce perturbative short-distance observables. In particular, we show that a rectangular array of 48 Rydberg atoms with existing quantum hardware capabilities should be able to adiabatically prepare low-energy states of the perturbatively matched theory. These states can then be used to simulate nonperturbative observables in the continuum limit that lie beyond the reach of classical computers.

DOI: 10.1103/PhysRevA.107.042404

I. INTRODUCTION

Future quantum simulations of Abelian and non-Abelian quantum field theories (QFTs), such as quantum chromodynamics (QCD), and descendant effective field theories will be important in developing robust predictive capabilities of the dynamics in a variety of physical systems of importance in high-energy and nuclear physics, ranging from the early universe, to highly inelastic processes in particle colliders, to the evolution of extreme astrophysical environments. Beyond the capabilities of classical computation, these challenges can only be addressed using yet-to-be-engineered quantum computers of sufficient capability [1,2]. During the last decade, rapid advances in the control of coherence and entanglement in the laboratory have led to the deployment of the first generation of quantum computing platforms, built around superconducting qubits [3–7], trapped ions [8], and neutral atoms [9–12]. These can be operated in a digital manner, where a universal gate set is used to emulate a specific Hamiltonian, or an analog manner, where the system is tuned to natively implement a target Hamiltonian, or as quantum annealers [13–15]. While digital quantum simulation platforms are universal in the sense that they can simulate an arbitrary Hamiltonian, the difficulties of implementing quantum gates have so far limited digital quantum simulations to relatively small systems. In contrast, analog quantum simulations have been performed with larger systems, but are limited by the native Hamiltonian of the experimental platform. Recent work has indicated that error rates on some analog simulation platforms are low enough for potential quantum advantages in physically interesting systems to be within reach [16]. In particular, cold-atom systems have been used to simulate the dynamics of quantum systems in regimes that are difficult for classical computers to simulate [17,18].

With the emerging potential of quantum computers, and the known limitations of classical computing, a growing effort is underway to develop efficient mappings of QFTs onto quantum computers, and the time evolution of an array of initial conditions. The asymptotic freedom of SU(2) and SU(3) gauge theories enables spatial lattice calculations to be perturbatively close to the continuum, and systematically correctable, as has long been used for lattice QCD classical simulations. Traditional lattice mappings of gauge theories, such as Kogut-Susskind [19], have led to first calculations of modest systems in low dimensions in U(1) [20–26], SU(2) [27–30], and SU(3) [31–35], and estimates of resource requirements, along with improved understandings about how to move forward. These advances have also driven the development of new and different encodings of QFTs onto finite discrete degrees of freedom [20–22,24–148].

Interestingly, the O(3) nonlinear sigma model (NLσM) in $1+1$ dimensions is a theory of interacting scalar particles that is asymptotically free and can support a topologically nontrivial ground state (vacuum). Because of these qualitative similarities with QCD, it serves as a useful test bed for the development of computational methods for QCD. A number of mappings of the O(3) NLσM suitable for quantum simulation have been introduced, including the Heisenberg comb, fuzzy sphere, angular momentum truncations and D-theory [132,149–153]. Previous work has shown that at lowest truncation, the fuzzy sphere regularization reproduces the O(3) NLσM [154], while the angular momentum truncation requires a larger local Hilbert space to do so [155]. The D-theory mapping with periodic boundary conditions (PBC) has been

[*]aciavare@uw.edu
[†]caspar@uw.edu
[‡]hershsg@uw.edu
[§]mjs5@uw.edu

shown in a number of works to reproduce the O(3) NLσM, both with and without a θ term [132,152,153]. However, present-day analog simulators, including arrays of cold atoms, only support open boundary conditions (OBC).

A central ingredient in lattice simulations of asymptotically free QFTs is the perturbative matching between the continuum and the lattice at short distances (compared to the scale at the theory becoming nonperturbative). In this work, it is shown that it is possible to perform this matching for the O(3) NLσM on existing analog quantum simulators. A definition of the renormalized coupling in the O(3) NLσM that is suitable to be used with OBC is introduced and implemented using tensor network simulations to compute the step-scaling function in the D-theory mapping. The step-scaling function is then matched to perturbative results at short distances (ultraviolet), and the results of Monte Carlo calculations at long distances (infrared), allowing for the minimum number of qubits required to reproduce continuum physics of the O(3) NLσM (to a given level of precision) to be determined. Tensor-network simulations indicate that asymptotic freedom and nonperturbative dynamics beyond the capabilities of classical computers in the O(3) NLσM can be potentially simulated with current cold-atom experimental configurations.

II. MAPPING D-THEORY TO QUBIT REGISTERS

The $1+1$D O(3) NLσM is defined by the action

$$S = \frac{1}{2g}\int dt\, dx\, \partial_\mu \vec{\phi}(x,t)\cdot\partial^\mu\vec{\phi}(x,t), \tag{1}$$

where $\vec{\phi}(x,t)$ is a vector of three scalar fields subject to the constraint $\vec{\phi}(x,t)\cdot\vec{\phi}(x,t)=1$. This constraint is responsible for transforming the free-boson action in Eq. (1) into an interacting asymptotically free QFT.

This theory has been extensively studied using classical Monte Carlo (MC) methods using a straightforward discretization of the above continuum action,

$$S_{\text{lat}} = -\frac{1}{g}\sum_{\langle ij\rangle}\vec{\phi}_i\cdot\vec{\phi}_j \ , \tag{2}$$

where the sum is over all nearest-neighbor sites i, j on a square Euclidean space-time lattice.

Simulating this theory on a quantum computer requires a truncation of the field, and the D-theory formulation provides a natural mapping onto qubit degrees of freedom and an intrinsic truncation utilizing dimensional reduction. In this mapping, spin-$\frac{1}{2}$ degrees of freedom are placed on a two-dimensional (2D) rectangular lattice of length L_x sites in the x direction and L_y sites in the y direction and coupled through an antiferromagnetic Heisenberg interaction, i.e.,

$$\hat{H}^D = J_x\sum_{x,y}\vec{S}_{x,y}\cdot\vec{S}_{x+1,y} + J_y\sum_{x,y}\vec{S}_{x,y}\cdot\vec{S}_{x,y+1} \ . \tag{3}$$

To obtain the $1+1$D O(3) NLσM, we choose J_x, J_y such that the 2D model is in a massless (symmetry broken) phase when $L_x, L_y \to \infty$. With this choice of parameters, the continuum limit of the NLσM is obtained in the limit $L_x \gg L_y \gg 1$, as has been demonstrated in several previous works for $J_x = J_y$ [132,152,153,156,157]. This has enabled classical Monte Carlo studies of the O(3) NLσM at finite density [156] and with a θ term [132] without a sign problem. In the isotropic ($J_x = J_y$) D-theory approach, each even L_y corresponds to a fixed coupling, and as the correlation length grows exponentially in L_y, this corresponds to a coarse set of lattice spacings. A more refined set of lattice spacings can be explored by varying J_x/J_y. In the regime $J_x/J_y \lesssim 1$, dimensional reduction should still occur, while the correlation length is reduced.

Determining the lattice spacing (in physical units) in any simulation of a QFT requires matching one or more dimensionful quantities calculated in lattice units to the corresponding experimentally or theoretically determined quantity. Such determinations have associated systematic errors due to the finite volume, imprecise input parameters, and other effects—see, for example, Ref. [158]. For the O(3) NLσM, the renormalized coupling can be used to set the length scale. Typically, Monte Carlo studies of the O(3) NLσM have been performed in a Euclidean space-time with PBC, and the renormalized coupling $\bar{g}(L)$ is defined in terms of two-point space-time correlation functions projected onto momentum modes [159]. This definition is somewhat problematic for our present purposes because quantum simulation platforms do not have direct access to Euclidean space-time correlation functions, and, further, it is more natural to implement OBC (for which momentum modes are no longer noninteracting eigenstates) on current platforms. Previous work has explored renormalized couplings defined in terms of energy gaps with OBC [154]. However, this is resource intensive to extract in practice on hardware, as it requires accurate preparation of both the ground state and first excited state and measurements of their energies. In this work, we introduce a different definition of $\bar{g}(L)$, given in terms of spatial correlations, that recovers the traditional definition in the perturbative regime, and which can be practically implemented in quantum simulations. Explicitly, $\bar{g}(L)$ is defined by

$$\bar{g}(L) = \frac{1}{2}\sqrt{\frac{1}{L\sin\left(\frac{\pi}{2L}\right)}\left(\frac{G_0}{G_1}-1\right)}, \tag{4}$$

where G_0 and G_1 are the largest and second-largest eigenvalues of the vacuum correlation matrix, G_{x_1,x_2}, defined by

$$G_{x_1,x_2} = \sum_{y_1,y_2}(-1)^{x_1+y_1+x_2+y_2}\,\langle\psi|\,\hat{S}^z_{x_1,y_1}\hat{S}^z_{x_2,y_2}\,|\psi\rangle\,, \tag{5}$$

where $|\psi\rangle$ is the vacuum state of the Hamiltonian in Eq. (3), and $\hat{S}^z_{x,y}$ is the z component of the spin operator at site (x,y). Recently, another method to extract the running coupling on quantum platforms for 2+1D quantum electrodynamics was proposed in Ref. [148], albeit with PBC.

To show that the continuum physics of the O(3) NLσM can be recovered on a quantum device, we compute a universal step-scaling function, $F_s(z)$, defined as

$$F_s(z) = s\frac{\bar{g}(sL, g_{\text{bare}})}{\bar{g}(L, g_{\text{bare}})}, \tag{6}$$

where $z = \bar{g}(L, g_{\text{bare}})$. Here, we emphasize that the bare coupling g_{bare} is kept fixed on the right-hand side. In the limit $z \to 0$, $F_s(z)$ probes infrared (IR) physics, and in the $z \to \infty$ limit, $F_s(z)$ probes ultraviolet (UV) physics. Therefore, if a lattice regularization reproduces the entire step-scaling function,

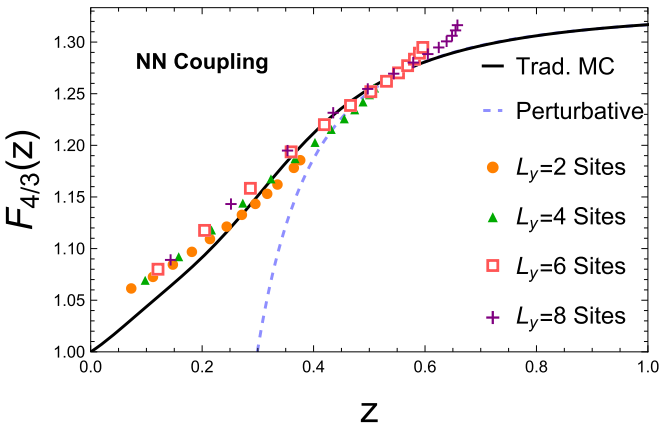

FIG. 1. The step-scaling function $F_{\frac{4}{3}}(z)$ for the coupling in Eq. (4) computed by varying $\frac{J_x}{J_y}$ for the nearest-neighbor (NN) D-theory Hamiltonian for going from a lattice of size $6 \times L_y$ sites to $8 \times L_y$ sites. The black line is a fit to results of Monte Carlo calculations using the traditional lattice regularization. The dashed blue line is the perturbative result [159].

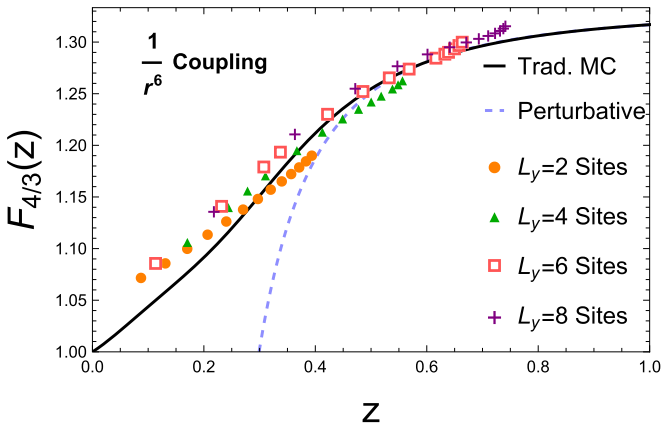

FIG. 2. The step-scaling function computed by varying $\frac{a_x}{a_y}$ for the $\frac{1}{r^6}$ D-theory Hamiltonian for going from a lattice of size $6 \times L_y$ sites to $8 \times L_y$ sites.

it can be said to reproduce the continuum physics of the O(3) NLσM. Any lattice regularization should be able to bridge the gap between perturbative UV physics and the nonperturbative IR physics. For simulations of asymptotically free theories, it is essential to match the lattice theory to the continuum theory (UV) with as few computational resources as possible, as the resulting nonperturbative IR physics emerges at parametrically larger length scales. To determine the size of lattices required to reproduce the O(3) NLσM, density matrix renormalization group (DMRG) calculations were performed using the C++ ITENSOR library [160,161] to obtain the vacuum state of the Hamiltonian in Eq. (3) for lattices of size $6 \times L_y$ and $8 \times L_y$ with OBC [161–164]. The renormalized couplings defined by Eq. (4) were used to compute $F_s(z)$ with $s = \frac{4}{3}$. Note that while traditionally $F_s(z)$ is computed for $s = 2$, any value of s may be used in principle, and we have used $s = \frac{4}{3}$ to reduce the classical computing overhead. Different points on the $F_{\frac{4}{3}}(z)$ curve, shown in Fig. 1, were computed by varying $\frac{J_x}{J_y}$ in the range $0.1 \leqslant \frac{J_x}{J_y} \leqslant 1.3$. At the lower end of the perturbative regime, $z \lesssim 0.55$, $F_s(z)$ is reproduced sufficiently well with $L_x = 6, 8$ lattice sites, provided a large transverse direction $L_y = 8$ is used. This indicates that perturbative matching between the continuum and lattice O(3) NLσM theories can be accomplished with as few as 64 qubits on a quantum device. While the D-theory Hamiltonian with nearest-neighbor couplings is natural to consider, some quantum simulation platforms, such as cold atoms, have long-range couplings. For example, arrays of Rydberg atoms with an s-wave coupling are described by a Hamiltonian with the form

$$\hat{H}^{\text{Ryd.}} = \sum_i \frac{\Omega_i(t)}{2} \hat{X}_i + \sum_i \Delta_i(t) \hat{n}_i + \sum_{i<j} \frac{C_6\, \hat{n}_i \hat{n}_j}{|\vec{x}_i - \vec{x}_j|^6}, \quad (7)$$

where $\hat{n}_i$ is the Rydberg-state occupation of atom i, $\vec{x}_i$ is the position of atom i, and $\hat{X}_i$ couples the ground state of atom i to its excited Rydberg state [9,10]. $\Omega_i(t)$ specifies the strength of the driving field at atom i, and $\Delta_i(t)$ specifies a local detuning. By identifying the excited-state occupation number with the z component of a spin, it can be seen that this system is described by an Ising Hamiltonian with long-range interactions and time-dependent external fields. Due to this native encoding of the Ising model, Rydberg atoms have been used in a number of studies to perform analog quantum simulations of the Ising model [17,18,165,166]. As we have shown in previous works, the Ising model with a strong transverse and longitudinal field can reproduce the dynamics of the Heisenberg model, and time-dependent external fields can be used to adiabatically prepare ground states of the Heisenberg model with long-range interactions [167,168]. In particular, by arranging atoms in a rectangular lattice and identifying the number operator of the atom at site (x, y), $\hat{n}_{x,y}$ with a staggered z component of a spin operator, i.e., $\hat{n}_{x,y} = \frac{1}{2} + (-1)^{x+y} \hat{S}^z_{x,y}$, it is possible to engineer a Heisenberg Hamiltonian,

$$\hat{H}^{\text{D6}} = \sum_{x_1,y_1,x_2,y_2} \frac{(-1)^{1+x_1+y_1+x_2+y_2}}{\left[a_x^2(x_1 - x_2)^2 + a_y^2(y_1 - y_2)^2\right]^3} \vec{S}_{x_1,y_1} \cdot \vec{S}_{x_2,y_2} \ , \quad (8)$$

where $a_{x,y}$ are the lattice spacings in the x, y directions. The staggered identification of the number operator with the spin operator is necessary to ensure that the state with all atoms in their ground state, in which the system will begin in a quantum simulation, corresponds to a state with staggered spins that is adiabatically connected to the ground state of Eq. (8). The staggering identification also makes the long-range interactions frustration free. Note that the Hamiltonian implemented on hardware will differ from that of Eq. (8) by a sign, but due to time-reversal symmetry this does not present an issue. This Hamiltonian is equivalent to the Hamiltonian in Eq. (3), with the addition of long-range frustration-free Heisenberg interactions. Therefore, it is expected that $a_{x,y}$ can be tuned so that dimensional reduction occurs and the low-energy degrees of freedom are described by the $1 + 1$D O(3) NLσM. To verify this, the step-scaling function for the vacuum state of this Hamiltonian was computed using DMRG, with the results shown in Fig. 2, where $\frac{a_y}{a_x}$ was varied in the range $0.1 \leqslant (\frac{a_y}{a_x})^6 \leqslant 1.3$. The step-scaling function computed with

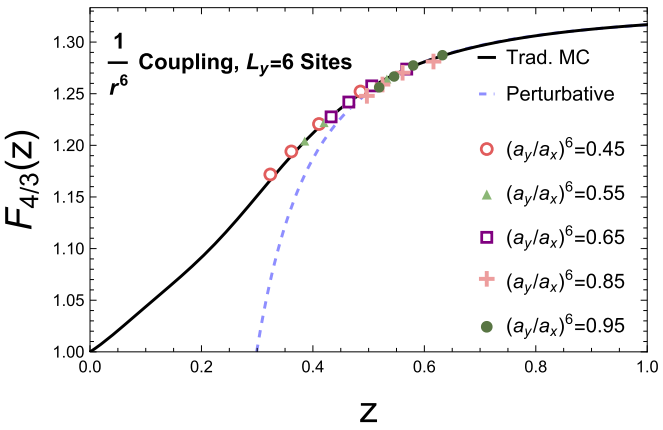

FIG. 3. The step-scaling function computed for $L_x = 6, 12, 18,$ and 24 sites with the $\frac{1}{r^6}$ D-theory Hamiltonian with $L_y = 6$ sites.

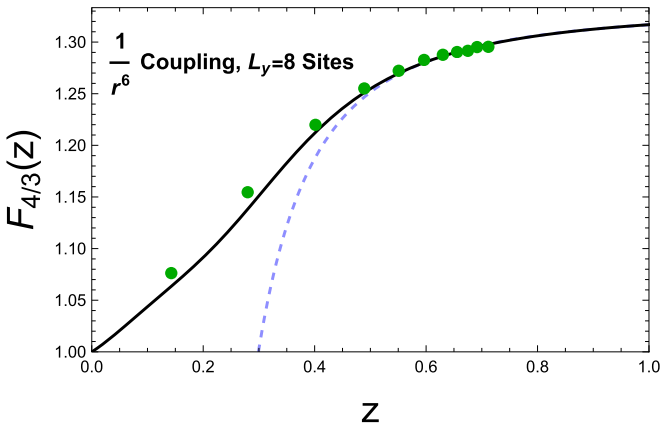

FIG. 4. $F_{4/3}(z)$ computed by varying $\frac{a_x}{a_y}$ for the $\frac{1}{r^6}$ D-theory Hamiltonian for going from a lattice of size 12×8 sites to 16×8 sites.

$L_y = 6$ reproduces the perturbative function over a range of parameters well into the perturbative regime, demonstrating that, for this range of couplings, the UV physics of the O(3) NLσM is correctly reproduced. It is interesting to note that $L_y = 6$ with nearest-neighbor couplings only is not able to reproduce the step-scaling function as precisely in this region, and in this sense, the $\frac{1}{r^6}$ coupling effectively implements an "improved" Hamiltonian that enables more precise matching with fewer qubits. However, $L_y = 6$ appears to be an optimum in this case, since $L_y = 8$ has again larger systematic errors for this L_x.

With controlled matching to the continuum theory, nonperturbative IR physics of the O(3) NLσM is expected to be able to be simulated by keeping the Hamiltonian parameters J_x, J_y, L_y fixed while increasing the lattice size L_x. To demonstrate that this procedure reproduces the IR correctly, $F_s(z)$ was computed with DMRG for lattices with larger L_x and $L_y = 6$, as shown in Fig. 3. $F_{\frac{4}{3}}(z)$ is correctly recovered in the nonperturbative regime as the lattice size is increased (when compared with the results of classical Monte Carlo calculations), over a wide range of anisotropy $0.45 \leqslant (a_y/a_x)^6 \leqslant 0.95$.

To match at scales further into the UV, lattices with larger L_y must be used. However, when $L_y > L_x$ it is possible for dimensional reduction to fail and the $1 + 1$D O(3) NLσM may not be reproduced, as is found for $L_y = 8$, where the results overshoot the Monte Carlo and perturbative step-scaling functions, as shown in Fig. 2. This can be remedied by using lattices with larger L_x. In Fig. 4, $F_{4/3}(z)$ from 12×8 to 16×8 lattices with the $\frac{1}{r^6}$ D-theory Hamiltonian is shown, which correctly reproduces the known result over a larger range than with the $L_y = 6$, $\frac{1}{r^6}$ D-theory Hamiltonian. This demonstrates how larger correlation lengths may be accessed, and hence the approach to the continuum limit.

III. QUANTUM SIMULATIONS OF O(3) NLσM USING RYDBERG ATOMS

Arrays of cold atoms are a promising platform for quantum simulation, and as shown above, modest lattice sizes of 6×6 and 8×6 are sufficient to reproduce the UV physics of the O(3) NLσM and demonstrate asymptotic freedom. This provides an opportunity for a first attempt at performing quantum simulations of nonperturbative (IR) dynamics of the O(3) NLσM. To do so will require the preparation of a low-energy state with respect to the Hamiltonian in Eq. (8). The adiabatic spiral [168] can be used to adiabatically prepare the ground state of this Hamiltonian on an array of cold atoms. To understand the quantum resources required to adiabatically prepare states with energy that is sufficiently low to reproduce low-lying physics of the O(3) NLσM, we performed time-dependent variational principle (TDVP) simulations of the adiabatic spiral using the C++ ITENSOR library [160,161,169–171]. Details of these calculations can be found in the Appendix. The classical simulations we performed assumed a rectangular array of ^{87}Rb atoms, with $C_6 = 5.42 \times 10^6$ MHz μm^6, with a vertical lattice spacing of 11 μm, and a selection of horizontal lattice spacings to probe different couplings. We assumed a maximum Rabi frequency of $\Omega = 25$ MHz, and a maximum coherence time of 4 μs. The initial state of the system with all atoms in their ground state corresponds to a Nèel state that is degenerate due to a symmetry under reflection of the spins. This degeneracy can be split by evolving with a global detuning term that is turned off during the course of the adiabatic evolution to apply an energy penalty. The initial size of the energy penalty was variationally optimized so that the renormalized coupling of the prepared state matched the vacuum state. The specific energy penalties and horizontal lattice spacings that we used are shown in Tables I and II. Results for the step scaling obtained from these simulations are shown in Fig. 5, where the uncertainties are derived from a sample of 5000 shots in computing the renormalized coupling for each lattice configuration.

These simulations show that an ideal cold-atom quantum simulator with only 48 atoms can correctly recover the UV physics of the O(3) NLσM with sufficient precision. To perform this quantum simulation in reality would require a rectangular array of ^{87}Rb atoms with a global driving field and a staggered detuning term. The parameters used in these simulations are close to those that have been implemented

TABLE I. Energy of the ground states prepared using the adiabatic spiral. The left column shows the lattice spacing used for the tensor network simulations of a 6×6 lattice. The center column shows the energy penalty used to match the vacuum renormalized coupling. The right column shows the energy of the state prepared by the adiabatic spiral in units of the Hamiltonian energy gap.

a_X (μm)	Energy penalty (MHz)	Final energy (Δ)
12.5	0.44	2.81
12.1	0.52	2.90
11.8	0.56	3.43
11.1	0.49	4.64

in previous cold-atom experiments [17,18,165,166,172]. Therefore, it is anticipated that analog quantum simulations of the O(3) NLσM should soon be within reach. Due to the similarity to previous cold-atom experiments, it is expected that these simulations can be performed with a high degree of fidelity. Scaling to larger systems will require the same pulse sequences applied to larger arrays of atoms. This is not expected to present an issue, as larger arrays of Rydberg atoms have been utilized in experiments [17,18,165] and the techniques used to simulate Heisenberg evolution have been shown to scale to large systems [167]. Note that while the simulations performed here are for arrays of ^{87}Rb atoms, similar calculations could be performed using different atomic species, such as Cs [173,174].

Reproducing the step-scaling curve shows that O(3) NLσM physics is actually being reproduced on the quantum simulator and is the first step towards achieving a quantum advantage in the simulation of the O(3) NLσM. Once an approximate vacuum state has been prepared on quantum hardware, particle wave packets can be excited by varying a local detuning or driving term. By exciting multiple particles in this manner, scattering in the O(3) NLσM can be directly simulated. Alternatively, all of this can also be done at a nonzero θ, by moving the atoms from a rectangular array into a staggered array [132]. Using dynamical reconfiguration of atoms, this could even be done dynamically, simulating a quench of the θ term. Rapidly turning on θ would correspond to a rapidly changing axion field, [175,176] and has been shown to generate a dynamical quantum phase transition in the context of lattice gauge theories [26,177]. Both of these

TABLE II. Energy of the ground states prepared using the adiabatic spiral. The left column shows the lattice spacing used for the tensor network simulations of a 8×6 lattice. The center column shows the energy penalty used to match the vacuum renormalized coupling. The right column shows the energy of the state prepared by the adiabatic spiral in units of the Hamiltonian energy gap.

a_X (μm)	Energy penalty (MHz)	Final energy (Δ)
12.5	0.3	4.52
12.1	0.4	4.56
11.8	0.46	5.43
11.1	0.45	7.52

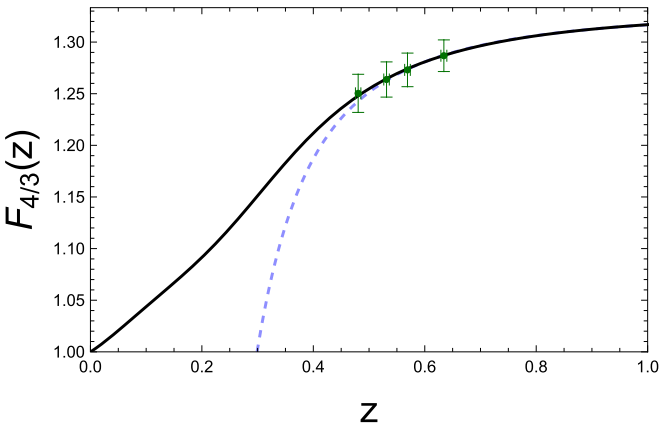

FIG. 5. Results for $F_{4/3}(z)$ computed in a TDVP simulation of a rectangular array of ^{87}Rb atoms assuming 5000 shots are used.

calculations involve real-time dynamics that have exponentially scaling computational costs on classical computers, and their successful simulation on a quantum computer could represent a true quantum advantage of scientific relevance to high-energy physics.

Note that these problems on the lattice sizes simulated in this section are within the reach of classical computers. Also, a true quantum advantage in simulations of the 1+1D O(3) NLσM will need to be performed with a choice of parameters that are outside the reach of perturbation theory. Based on Fig. 3, performing these simulations on a lattice of size 18×6 with $(a_y/a_x)^6 = 0.45$ is a potential candidate for quantum advantage. A lattice of this size is outside the reach of state vector simulation and lies in the nonperturbative region of the step-scaling curve. The DMRG calculations to produce Fig. 3 required a bond dimension of 2000 to converge, and simulating scattering dynamics or a θ quench will involve an exponentially growing bond dimension beyond this. Note, however, that some tensor networks more suited to two dimensions such as PEPS may be able to perform this calculation with a lower bond dimension. Regardless, a simulation on this lattice size will be in a regime that is difficult for classical computers and would represent a first chance at seeing a quantum advantage.

IV. DISCUSSION

A challenging path lies ahead for the quantum simulation of physical systems of importance in high-energy and nuclear physics. Both Abelian and non-Abelian gauge theories must be mapped efficiently onto quantum computers, and it remains to be determined which of the known frameworks, if any, will evolve toward providing robust predictive capabilities. For strong interactions, asymptotic freedom has been key in enabling nonperturbative classical calculations with lattice QCD of near-static quantities, and much of the associated technology will translate across to quantum simulations. In this work, we have studied a different asymptotically free field theory. By developing new methods and performing classical simulations, we have shown that present-day analog quantum simulators have the potential to perform quantum simula-

tions of nonperturbative dynamics within this QFT with fully quantifiable uncertainties. A definition of the renormalized coupling for the 1+1D O(3) NLσM with OBC was developed to enable the first perturbative matching of lattice calculations on quantum simulators to the continuum. It is expected that this will enable the use of quantum simulators to compute quantities of interest in the continuum limit of the 1+1D O(3) NLσM. Additionally, this definition was used to determine the minimal number of qubits required for a quantum computer to reproduce continuum physics. Remarkably, a cold-atom quantum simulator only needs a rectangular array of 48 atoms to begin to quantitatively reproduce nonperturbative dynamics within the O(3) NLσM. Cold atoms have been previously used to simulate larger systems, and tensor network simulations suggest that existing cold-atom experiments should be capable of demonstrating the asymptotic freedom of the O(3) NLσM. We have also shown that the long-range coupling present in cold-atom quantum simulators enables them to make contact with the continuum physics of the O(3) NLσM with fewer qubits than mappings that are restricted to nearest-neighbor couplings. This is the first concrete example of an "improved" Hamiltonian that reduces the qubit count required for a quantum simulation of a lattice field theory to rigorously simulate continuum physics with controlled uncertainties.

While the 1+1D O(3) NLσM does not describe any of the fundamental forces in nature, it does share a number of qualitative aspects with QCD, so these simulations will provide valuable insights into how to perform quantum simulations of standard model physics. Our calculations correctly recover the classically computed step-scaling function, and demonstrate that the continuum O(3) NLσM is being matched, within tolerances, to lattices, and provides new and valuable further steps toward rigorously extracting information about a continuum QFT from quantum computers. Once matching has been performed, a quantum computer can be used to simulate nonperturbative quantities in the theory that are beyond the reach of classical computers, including scattering and fragmentation, and θ quenches. Further, the D-theory mapping studied in this work has the potential to be used to simulate the O(3) NLσM in $2+1$ dimensions by making use of 3D cold-atom arrays which have recently been experimentally demonstrated [11].

ACKNOWLEDGMENTS

We would like to thank Pavel Lougovski and Peter Komar from the AWS Braket team for useful discussions. The views expressed are those of the authors and do not reflect the official policy or position of AWS. We would also like to thank Henry Froland and Nikita Zemlevskiy for helpful discussions. This work was supported in part by U.S. Department of Energy, Office of Science, Office of Nuclear Physics, Inqubator for Quantum Simulation (IQuS) under DOE (NP) Award No. DE-SC0020970, in part by the DOE QuantISED program through the theory consortium "Intersections of QIS and Theoretical Particle Physics" at Fermilab with Fermilab Subcontract No. 666484, and in part by Institute for Nuclear Theory with DOE Grant No. DE-FG02-00ER41132. This work was enabled in part by the use of advanced computational, storage, and networking infrastructure provided by the Hyak supercomputer system at the University of Washington [178]. This work was also supported in part through the Department of Physics [179] and the College of Arts and Sciences [180] at the University of Washington. This work also made use of AWS EC-2 compute instances through the generous support of AWS Programs for Research and Education.

APPENDIX: RYDBERG ATOM SIMULATION

The Hamiltonian describing the evolution of a rectangular array of Rydberg atoms is

$$\hat{H}^{\text{Ryd.}}(t) = \sum_{x_1,y_1,x_2,y_2} \frac{C_6\ \hat{n}_{x_1,y_1}\hat{n}_{x_2,y_2}}{\left[a_x^2(x_1-x_2)^2 + a_y^2(y_1-y_2)^2\right]^3} + \sum_{x,y} \Delta_{x,y}(t)\hat{n}_{x,y} + \sum_{x,y} \frac{\Omega_{x,y}(t)}{2}\hat{X}_{x,y}, \tag{A1}$$

where $\hat{n}_{x,y}$ is the Rydberg occupation number, $\Delta_{x,y}(t)$ is a position-dependent detuning term, $\Omega_{x,y}(t)$ is a position-dependent driving term, a_x is the horizontal lattice spacing, and a_y is the vertical lattice spacing. As presented in the main text, the Rydberg number operator can be identified with a staggered spin operator, i.e., $\hat{n}_{x,y} = \frac{1}{2} + (-1)^{x+y}\hat{S}^z_{x,y}$, such that the state with all atoms in their ground state corresponds to a Néel state. With this identification, the adiabatic spiral introduced in Ref. [168] can be used to prepare a low-energy state of the Hamiltonian in Eq. (8), by using

$$\begin{aligned}\Delta_{x,y}(t) &= (-1)^{x+y}\Omega_D + h_P\left(1-\frac{t}{T}\right) + \frac{1}{2}\sum_{(x_2,y_2)\neq(x,y)} \frac{C_6}{\left[a_x^2(x-x_2)^2 + a_y^2(y-y_2)^2\right]^3},\\ \Omega_{x,y}(t) &= \sqrt{2}\,\Omega_D\left[\frac{t}{T} + \frac{1}{\pi}\sin\left(\pi\frac{t}{T}\right)\right],\end{aligned} \tag{A2}$$

where h_P is an initial energy penalty, Ω_D specifies the final strength of the driving field, and T is the total time used for the adiabatic state preparation. For our calculations, we have used $\Omega_D = \frac{1}{\sqrt{2}}25$ MHz, $T = 3.83$ μs, and h_P is presented in Tables I and II. Performing a measurement on a Rydberg atom simulator requires the drive field to be turned off, which we simulated by quenching $\Omega_{x,y}(t)$ to zero over a time interval of 0.1 μs. We assumed that a combined time of 0.07 μs was required to turn the detuning on and off.

The adiabatic spiral described here was simulated with tensor networks. This was done with the C++ ITENSOR library with OPENBLAS as the backend to parallelize the linear algebra operations [161]. The state of the system was represented with a matrix product states (MPS) tensor that wound through the 2D lattice. Time evolution was performed by discretizing $\hat{H}^{\text{Ryd.}}(t)$ into 200 time-independent steps and evolving with one-site TDVP [169,170]. Before each step, the bond dimension was increased using the global Krylov method [171], with a maximum allowed bond dimension of 550.

[1] R. P. Feynman, Simulating physics with computers, Int. J. Theor. Phys. **21**, 467 (1982).

[2] P. Benioff, The computer as a physical system: A microscopic quantum mechanical hamiltonian model of computers as represented by turing machines, J. Stat. Phys. **22**, 563 (1980).

[3] H. L. Huang, D. Wu, D. Fan, and X. Zhu, Superconducting quantum computing a review, Sci. China Info. Sci. **63**, 180501 (2020).

[4] R. Bianchetti, S. Filipp, M. Baur, J. M. Fink, C. Lang, L. Steffen, M. Boissonneault, A. Blais, and A. Wallraff, Control and Tomography of a Three Level Superconducting Artificial Atom, Phys. Rev. Lett. **105**, 223601 (2010).

[5] C. Wang, I. Gonin, A. Grassellino, S. Kazakov, A. Romanenko, V. P. Yakovlev, and S. Zorzetti, High-efficiency microwave optical quantum transduction based on a cavity electro-optic superconducting system with long coherence time, npj Quantum Info. **8**, 149 (2022)..

[6] A. Wallraff, D. I. Schuster, A. Blais, L. Frunzio, R.-S. Huang, J. Majer, S. Kumar, S. M. Girvin, and R. J. Schoelkopf, Strong coupling of a single photon to a superconducting qubit using circuit quantum electrodynamics, Nature (London) **431**, 162 (2004).

[7] I. Chiorescu, P. Bertet, K. Semba, Y. Nakamura, C. Harmans, and J. Mooij, Coherent dynamics of a flux qubit coupled to a harmonic oscillator, Nature (London) **431**, 159 (2004).

[8] C. D. Bruzewicz, J. Chiaverini, R. McConnell, and J. M. Sage, Trapped-ion quantum computing: Progress and challenges, Appl. Phys. Rev. **6**, 021314 (2019).

[9] L. Henriet, L. Beguin, A. Signoles, T. Lahaye, A. Browaeys, G.-O. Reymond, and C. Jurczak, Quantum computing with neutral atoms, Quantum **4**, 327 (2020).

[10] A. Browaeys and T. Lahaye, Many-body physics with individually controlled Rydberg atoms, Nat. Phys. **16**, 132 (2020).

[11] D. Barredo, V. Lienhard, P. Scholl, S. de Lé séleuc, T. Boulier, A. Browaeys, and T. Lahaye, Three-Dimensional Trapping of Individual Rydberg Atoms in Ponderomotive Bottle Beam Traps, Phys. Rev. Lett. **124**, 023201 (2020).

[12] D. Bluvstein, H. Levine, G. Semeghini, T. T. Wang, S. Ebadi, M. Kalinowski, A. Keesling, N. Maskara, H. Pichler, M. Greiner *et al.*, A quantum processor based on coherent transport of entangled atom arrays, Nature (London) **604**, 451 (2022).

[13] M. W. Johnson, M. H. Amin, S. Gildert, T. Lanting, F. Hamze, N. Dickson, R. Harris, A. J. Berkley, J. Johansson, P. Bunyk *et al.*, Quantum annealing with manufactured spins, Nature (London) **473**, 194 (2011).

[14] R. Harris, M. W. Johnson, T. Lanting, A. J. Berkley, J. Johansson, P. Bunyk, E. Tolkacheva, E. Ladizinsky, N. Ladizinsky, T. Oh, F. Cioata, I. Perminov, P. Spear, C. Enderud, C. Rich, S. Uchaikin, M. C. Thom, E. M. Chapple, J. Wang, B. Wilson *et al.*, Experimental investigation of an eight-qubit unit cell in a superconducting optimization processor, Phys. Rev. B **82**, 024511 (2010).

[15] P. I. Bunyk, E. M. Hoskinson, M. W. Johnson, E. Tolkacheva, F. Altomare, A. J. Berkley, R. Harris, J. P. Hilton, T. Lanting, A. J. Przybysz, and J. Whittaker, Architectural considerations in the design of a superconducting quantum annealing processor, IEEE Trans. Appl. Supercond. **24**, 1 (2014).

[16] S. Flannigan, N. Pearson, G. H. Low, A. Buyskikh, I. Bloch, P. Zoller, M. Troyer, and A. J. Daley, Propagation of errors and quantitative quantum simulation with quantum advantage, Quantum Sci. Techno. **7**, 045025 (2022).

[17] S. Ebadi, T. T. Wang, H. Levine, A. Keesling, G. Semeghini, A. Omran, D. Bluvstein, R. Samajdar, H. Pichler, W. W. Ho *et al.*, Quantum phases of matter on a 256-atom programmable quantum simulator, Nature (London) **595**, 227 (2021).

[18] P. Scholl, M. Schuler, H. J. Williams, A. A. Eberharter, D. Barredo, K.-N. Schymik, V. Lienhard, L.-P. Henry, T. C. Lang, T. Lahaye, A. M. Läuchli, and A. Browaeys, Quantum simulation of 2D antiferromagnets with hundreds of Rydberg atoms, Nature (London) **595**, 233 (2021).

[19] J. Kogut and L. Susskind, Hamiltonian formulation of Wilson's lattice gauge theories, Phys. Rev. D **11**, 395 (1975).

[20] E. A. Martinez, C. A. Muschik, P. Schindler, D. Nigg, A. Erhard, M. Heyl, P. Hauke, M. Dalmonte, T. Monz, P. Zoller, and R. Blatt, Real-time dynamics of lattice gauge theories with a few-qubit quantum computer, Nature (London) **534**, 516 (2016).

[21] N. Klco, E. F. Dumitrescu, A. J. McCaskey, T. D. Morris, R. C. Pooser, M. Sanz, E. Solano, P. Lougovski, and M. J. Savage, Quantum-classical computation of Schwinger model dynamics using quantum computers, Phys. Rev. A **98**, 032331 (2018).

[22] H.-H. Lu, N. Klco, J. M. Lukens, T. D. Morris, A. Bansal, A. Ekström, G. Hagen, T. Papenbrock, A. M. Weiner, M. J. Savage, and P. Lougovski, Simulations of subatomic many-body physics on a quantum frequency processor, Phys. Rev. A **100**, 012320 (2019).

[23] F. M. Surace, P. P. Mazza, G. Giudici, A. Lerose, A. Gambassi, and M. Dalmonte, Lattice Gauge Theories and String Dynamics in Rydberg Atom Quantum Simulators, Phys. Rev. X **10**, 021041 (2020).

[24] N. H. Nguyen, M. C. Tran, Y. Zhu, A. M. Green, C. H. Alderete, Z. Davoudi, and N. M. Linke, Digital quantum simulation of the Schwinger model and symmetry protection with trapped ions, PRX Quantum **3**, 020324 (2022).

[25] S. Thompson and G. Siopsis, Quantum computation of phase transition in the massive Schwinger model, Quantum Sci. Technol. **7**, 035001 (2022).

[26] T. V. Zache, N. Mueller, J. T. Schneider, F. Jendrzejewski, J. Berges, and P. Hauke, Dynamical Topological Transitions in the Massive Schwinger Model with a θ Term, Phys. Rev. Lett. **122**, 050403 (2019).

[27] N. Klco, M. J. Savage, and J. R. Stryker, SU(2) non-Abelian gauge field theory in one dimension on digital quantum computers, Phys. Rev. D **101**, 074512 (2020).

[28] S. A Rahman, R. Lewis, E. Mendicelli, and S. Powell, SU(2) lattice gauge theory on a quantum annealer, Phys. Rev. D **104**, 034501 (2021).

[29] Y. Y. Atas, J. Zhang, R. Lewis, A. Jahanpour, J. F. Haase, and C. A. Muschik, SU(2) hadrons on a quantum computer via a variational approach, Nat. Commun. **12**, 6499 (2021).

[30] S. A. Rahman, R. Lewis, E. Mendicelli, and S. Powell, Self-mitigating Trotter circuits for SU(2) lattice gauge theory on a quantum computer, Phys. Rev. D **106**, 074502 (2022).

[31] A. Ciavarella, N. Klco, and M. J. Savage, Trailhead for quantum simulation of SU(3) Yang-Mills lattice gauge theory in the local multiplet basis, Phys. Rev. D **103**, 094501 (2021).

[32] A. N. Ciavarella and I. A. Chernyshev, Preparation of the SU(3) lattice Yang-Mills vacuum with variational quantum methods, Phys. Rev. D **105**, 074504 (2022).
[33] R. C. Farrell, I. A. Chernyshev, S. J. M. Powell, N. A. Zemlevskiy, M. Illa, and M. J. Savage, Preparations for quantum simulations of quantum chromodynamics in 1+1 dimensions: (I) Axial gauge, arXiv:2207.01731.
[34] R. C. Farrell, I. A. Chernyshev, S. J. M. Powell, N. A. Zemlevskiy, M. Illa, and M. J. Savage, Preparations for quantum simulations of quantum chromodynamics in 1+1 dimensions: (II) Single-baryon beta-decay in real time, arXiv:2209.10781.
[35] Y. Y. Atas, J. F. Haase, J. Zhang, V. Wei, S. M. L. Pfaendler, R. Lewis, and C. A. Muschik, Real-time evolution of SU(3) hadrons on a quantum computer, arXiv:2207.03473.
[36] R. Brower, S. Chandrasekharan, and U. J. Wiese, QCD as a quantum link model, Phys. Rev. D **60**, 094502 (1999).
[37] T. Byrnes and Y. Yamamoto, Simulating lattice gauge theories on a quantum computer, Phys. Rev. A **73**, 022328 (2006).
[38] E. Zohar and B. Reznik, Confinement and Lattice Quantum-Electrodynamic Electric Flux Tubes Simulated with Ultracold Atoms, Phys. Rev. Lett. **107**, 275301 (2011).
[39] E. Zohar, J. I. Cirac, and B. Reznik, Simulating Compact Quantum Electrodynamics with Ultracold Atoms: Probing Confinement and Nonperturbative Effects, Phys. Rev. Lett. **109**, 125302 (2012).
[40] L. Tagliacozzo, A. Celi, A. Zamora, and M. Lewenstein, Optical Abelian lattice gauge theories, Ann. Phys. **330**, 160 (2013).
[41] D. Banerjee, M. Bögli, M. Dalmonte, E. Rico, P. Stebler, U. J. Wiese, and P. Zoller, Atomic Quantum Simulation of U(N) and SU(N) Non-Abelian Lattice Gauge Theories, Phys. Rev. Lett. **110**, 125303 (2013).
[42] L. Tagliacozzo, A. Celi, P. Orland, and M. Lewenstein, Simulations of non-Abelian gauge theories with optical lattices, Nat. Commun. **4**, 2615 (2013).
[43] E. Zohar, J. I. Cirac, and B. Reznik, Cold-Atom Quantum Simulator for SU(2) Yang-Mills Lattice Gauge Theory, Phys. Rev. Lett. **110**, 125304 (2013).
[44] E. Zohar, J. I. Cirac, and B. Reznik, Simulating (2+1)-Dimensional Lattice QED with Dynamical Matter Using Ultracold Atoms, Phys. Rev. Lett. **110**, 055302 (2013).
[45] U.-J. Wiese, Ultracold quantum gases and lattice systems: Quantum simulation of lattice gauge theories, Ann. Phys. **525**, 777 (2013).
[46] P. Hauke, D. Marcos, M. Dalmonte, and P. Zoller, Quantum Simulation of a Lattice Schwinger Model in a Chain of Trapped Ions, Phys. Rev. X **3**, 041018 (2013).
[47] D. Marcos, P. Widmer, E. Rico, M. Hafezi, P. Rabl, U. J. Wiese, and P. Zoller, Two-dimensional lattice gauge theories with superconducting quantum circuits, Ann. Phys. **351**, 634 (2014).
[48] Y. Kuno, K. Kasamatsu, Y. Takahashi, I. Ichinose, and T. Matsui, Real-time dynamics and proposal for feasible experiments of lattice gauge–Higgs model simulated by cold atoms, New J. Phys. **17**, 063005 (2015).
[49] A. Bazavov, Y. Meurice, S.-W. Tsai, J. Unmuth-Yockey, and J. Zhang, Gauge-invariant implementation of the Abelian Higgs model on optical lattices, Phys. Rev. D **92**, 076003 (2015).
[50] V. Kasper, F. Hebenstreit, M. Oberthaler, and J. Berges, Schwinger pair production with ultracold atoms, Phys. Lett. B **760**, 742 (2016).
[51] G. K. Brennen, G. Pupillo, E. Rico, T. M. Stace, and D. Vodola, Loops and Strings in a Superconducting Lattice Gauge Simulator, Phys. Rev. Lett. **117**, 240504 (2016).
[52] Y. Kuno, S. Sakane, K. Kasamatsu, I. Ichinose, and T. Matsui, Atomic quantum simulation of a three-dimensional U(1) gauge-Higgs model, Phys. Rev. A **94**, 063641 (2016).
[53] E. Zohar, A. Farace, B. Reznik, and J. I. Cirac, Digital lattice gauge theories, Phys. Rev. A **95**, 023604 (2017).
[54] V. Kasper, F. Hebenstreit, F. Jendrzejewski, M. K. Oberthaler, and J. Berges, Implementing quantum electrodynamics with ultracold atomic systems, New J. Phys. **19**, 023030 (2017).
[55] C. Muschik, M. Heyl, E. Martinez, T. Monz, P. Schindler, B. Vogell, M. Dalmonte, P. Hauke, R. Blatt, and P. Zoller, U(1) Wilson lattice gauge theories in digital quantum simulators, New J. Phys. **19**, 103020 (2017).
[56] D. González-Cuadra, E. Zohar, and J. I. Cirac, Quantum simulation of the Abelian-Higgs lattice gauge theory with ultracold atoms, New J. Phys. **19**, 063038 (2017).
[57] M. C. Bañuls, K. Cichy, J. I. Cirac, K. Jansen, and S. Kühn, Efficient Basis Formulation for (1+1Dimensional SU(2) Lattice Gauge Theory: Spectral Calculations with Matrix Product States, Phys. Rev. X **7**, 041046 (2017).
[58] E. F. Dumitrescu, A. J. McCaskey, G. Hagen, G. R. Jansen, T. D. Morris, T. Papenbrock, R. C. Pooser, D. J. Dean, and P. Lougovski, Cloud Quantum Computing of an Atomic Nucleus, Phys. Rev. Lett. **120**, 210501 (2018).
[59] D. B. Kaplan and J. R. Stryker, Gauss's law, duality, and the Hamiltonian formulation of U(1) lattice gauge theory, Phys. Rev. D **102**, 094515 (2020).
[60] C. Kokail, C. Maier, R. van Bijnen, T. Brydges, M. K. Joshi, P. Jurcevic, C. A. Muschik, P. Silvi, R. Blatt, C. F. Roos, and P. Zoller, Self-verifying variational quantum simulation of lattice models, Nature (London) **569**, 355 (2019).
[61] K. Yeter-Aydeniz, E. F. Dumitrescu, A. J. McCaskey, R. S. Bennink, R. C. Pooser, and G. Siopsis, Scalar quantum field theories as a benchmark for near-term quantum computers, Phys. Rev. A **99**, 032306 (2019).
[62] J. R. Stryker, Oracles for Gauss's law on digital quantum computers, Phys. Rev. A **99**, 042301 (2019).
[63] E. Gustafson, Y. Meurice, and J. Unmuth-Yockey, Quantum simulation of scattering in the quantum Ising model, Phys. Rev. D **99**, 094503 (2019).
[64] I. C. Clöet, M. R. Dietrich, J. Arrington, A. Bazavov, M. Bishof, A. Freese, A. V. Gorshkov, A. Grassellino, K. Hafidi, Z. Jacob *et al.*, Opportunities for nuclear physics & quantum information science, arXiv:1903.05453.
[65] B. Nachman, D. Provasoli, W. A. de Jong, and C. W. Bauer, Quantum Algorithm for High Energy Physics Simulations, Phys. Rev. Lett. **126**, 062001 (2021).
[66] O. Shehab, K. A. Landsman, Y. Nam, D. Zhu, N. M. Linke, M. J. Keesan, R. C. Pooser, and C. R. Monroe, Toward convergence of effective field theory simulations on digital quantum computers, Phys. Rev. A **100**, 062319 (2019).
[67] N. Klco and M. J. Savage, Minimally entangled state preparation of localized wave functions on quantum computers, Phys. Rev. A **102**, 012612 (2020).

[68] A. Alexandru, P. F. Bedaque, S. Harmalkar, H. Lamm, S. Lawrence, and N. C. Warrington (NuQS Collaboration), Gluon field digitization for quantum computers, Phys. Rev. D **100**, 114501 (2019).

[69] Z. Davoudi, M. Hafezi, C. Monroe, G. Pagano, A. Seif, and A. Shaw, Towards analog quantum simulations of lattice gauge theories with trapped ions, Phys. Rev. Res. **2**, 023015 (2020).

[70] A. Avkhadiev, P. E. Shanahan, and R. D. Young, Accelerating Lattice Quantum Field Theory Calculations via Interpolator Optimization Using Noisy Intermediate-Scale Quantum Computing, Phys. Rev. Lett. **124**, 080501 (2020).

[71] G. Magnifico, M. Dalmonte, P. Facchi, S. Pascazio, F. V. Pepe, and E. Ercolessi, Real time dynamics and confinement in the $\mathbb{Z}_n$ Schwinger-Weyl lattice model for 1+1 QED, Quantum **4**, 281 (2020).

[72] E. Gustafson, P. Dreher, Z. Hang, and Y. Meurice, Indexed improvements for real-time trotter evolution of a (1 + 1) field theory using NISQ quantum computers, Quantum Sci. Technol. **6**, 045020 (2021).

[73] M. C. Bañuls, R. Blatt, J. Catani, A. Celi, J. I. Cirac, M. Dalmonte, L. Fallani, K. Jansen, M. Lewenstein, S. Montangero, C. A. Muschik, B. Reznik, E. Rico, L. Tagliacozzo, K. V. Acoleyen, F. Verstraete, U.-J. Wiese, M. Wingate, J. Zakrzewski, and P. Zoller, Simulating lattice gauge theories within quantum technologies, Eur. Phys. J. D **74**, 165 (2020).

[74] N. Klco and M. J. Savage, Systematically localizable operators for quantum simulations of quantum field theories, Phys. Rev. A **102**, 012619 (2020).

[75] C. Mishra, S. Thompson, R. Pooser, and G. Siopsis, Quantum computation of an interacting fermionic model, Quantum Sci. Technol. **5**, 035010 (2020).

[76] D. Luo, J. Shen, M. Highman, B. K. Clark, B. DeMarco, A. X. El-Khadra, and B. Gadway, Framework for simulating gauge theories with dipolar spin systems, Phys. Rev. A **102**, 032617 (2020).

[77] D. E. Kharzeev and Y. Kikuchi, Real-time chiral dynamics from a digital quantum simulation, Phys. Rev. Res. **2**, 023342 (2020).

[78] N. Mueller, A. Tarasov, and R. Venugopalan, Computing real time correlation functions on a hybrid classical/quantum computer, Nucl. Phys. A **1005**, 121889 (2021).

[79] A. F. Shaw, P. Lougovski, J. R. Stryker, and N. Wiebe, Quantum algorithms for simulating the lattice Schwinger model, Quantum **4**, 306 (2020).

[80] B. Yang, H. Sun, R. Ott, H.-Y. Wang, T. V. Zache, J. C. Halimeh, Z.-S. Yuan, P. Hauke, and J.-W. Pan, Observation of gauge invariance in a 71-site Bose-Hubbard quantum simulator, Nature (London) **587**, 392 (2020).

[81] Y. Ji, H. Lamm, and S. Zhu (NuQS), Gluon field digitization via group space decimation for quantum computers, Phys. Rev. D **102**, 114513 (2020).

[82] J. Bender, P. Emonts, E. Zohar, and J. I. Cirac, Real-time dynamics in 2 + 1D compact QED using complex periodic Gaussian states, Phys. Rev. Res. **2**, 043145 (2020).

[83] J. F. Haase, L. Dellantonio, A. Celi, D. Paulson, A. Kan, K. Jansen, and C. A. Muschik, A resource efficient approach for quantum and classical simulations of gauge theories in particle physics, Quantum **5**, 393 (2021).

[84] J. C. Halimeh, H. Lang, J. Mildenberger, Z. Jiang, and P. Hauke, Gauge-symmetry protection using single-body terms, PRX Quantum **2**, 040311 (2021).

[85] D. Robaina, M. C. Bañuls, and J. I. Cirac, Simulating $2 + 1DZ_3$ Lattice Gauge Theory with an Infinite Projected Entangled-Pair State, Phys. Rev. Lett. **126**, 050401 (2021).

[86] K. Yeter-Aydeniz, G. Siopsis, and R. C. Pooser, Scattering in the Ising model with the quantum Lanczos algorithm, New J. Phys. **23**, 043033 (2021).

[87] D. Paulson, L. Dellantonio, J. F. Haase, A. Celi, A. Kan, A. Jena, C. Kokail, R. van Bijnen, K. Jansen, P. Zoller, and C. A. Muschik, Towards simulating 2D effects in lattice gauge theories on a quantum computer, PRX Quantum **2**, 030334 (2021).

[88] J. C. Halimeh, V. Kasper, and P. Hauke, Fate of lattice gauge theories under decoherence, arXiv:2009.07848.

[89] M. Van Damme, J. C. Halimeh, and P. Hauke, Gauge-Symmetry Violation Quantum Phase Transition in Lattice Gauge Theories, arXiv:2010.07338.

[90] J. Barata, N. Mueller, A. Tarasov, and R. Venugopalan, Single-particle digitization strategy for quantum computation of a ϕ^4 scalar field theory, Phys. Rev. A **103**, 042410 (2021).

[91] A. Milsted, J. Liu, J. Preskill, and G. Vidal, Collisions of false-vacuum bubble walls in a quantum spin chain, PRX Quantum **3**, 020316 (2022).

[92] V. Kasper, T. V. Zache, F. Jendrzejewski, M. Lewenstein, and E. Zohar, Non-abelian gauge invariance from dynamical decoupling, Phys. Rev. D **107**, 014506 (2023).

[93] R. Ott, T. V. Zache, F. Jendrzejewski, and J. Berges, Scalable Cold-Atom Quantum Simulator for Two-Dimensional QED, Phys. Rev. Lett. **127**, 130504 (2021).

[94] C. W. Bauer, B. Nachman, and M. Freytsis, Simulating Collider Physics on Quantum Computers Using Effective Field Theories, Phys. Rev. Lett. **127**, 212001 (2021).

[95] E. Gustafson, Y. Zhu, P. Dreher, N. M. Linke, and Y. Meurice, Real-time quantum calculations of phase shifts using wave packet time delays, Phys. Rev. D **104**, 054507 (2021).

[96] K. Yeter-Aydeniz, S. Bangar, G. Siopsis, and R. C. Pooser, Collective neutrino oscillations on a quantum computer, Quant. Inf. Proc. **21**, 84 (2022).

[97] Z. Davoudi, N. M. Linke, and G. Pagano, Toward simulating quantum field theories with controlled phonon-ion dynamics: A hybrid analog-digital approach, Phys. Rev. Res. **3**, 043072 (2021).

[98] A. Kan, L. Funcke, S. Kühn, L. Dellantonio, J. Zhang, J. F. Haase, C. A. Muschik, and K. Jansen, Investigating a 3+1D topological θ-term in the Hamiltonian formulation of lattice gauge theories for quantum and classical simulations, Phys. Rev. D **104**, 034504 (2021).

[99] J. R. Stryker, Shearing approach to gauge invariant Trotterization, arXiv:2105.11548.

[100] M. Aidelsburger, L. Barbiero, A. Bermudez, T. Chanda, A. Dauphin, D. González-Cuadra, P. R. Grzybowski, S. Hands, F. Jendrzejewski, J. Jünemann, G. Juzeliunas, V. Kasper, A. Piga, S.-J. Ran, M. Rizzi, G. Sierra, L. Tagliacozzo, E. Tirrito, T. V. Zache, J. Zakrzewski *et al.*, Cold atoms meet lattice gauge theory, Philos. Trans. R. Soc. London A **380**, 20210064 (2021).

[101] E. Zohar, Quantum simulation of lattice gauge theories in more than one space dimension—Requirements, challenges

and methods, Philos. Trans. A. Math. Phys. Eng. Sci. **380**, 20210069 (2021).

[102] J. C. Halimeh, H. Lang, and P. Hauke, Gauge protection in non-Abelian lattice gauge theories, New J. Phys. **24**, 033015 (2022).

[103] K. Yeter-Aydeniz, E. Moschandreou, and G. Siopsis, Quantum imaginary-time evolution algorithm for quantum field theories with continuous variables, Phys. Rev. A **105**, 012412 (2022).

[104] J. Knaute and P. Hauke, Relativistic meson spectra on ion-trap quantum simulators, Phys. Rev. A **105**, 022616 (2022).

[105] U.-J. Wiese, From quantum link models to D-theory: A resource efficient framework for the quantum simulation and computation of gauge theories, Philos. Trans. A. Math. Phys. Eng. Sci. **380**, 20210068 (2021).

[106] Y. Meurice, Theoretical methods to design and test quantum simulators for the compact Abelian Higgs model, Phys. Rev. D **104**, 094513 (2021).

[107] N. Mueller, T. V. Zache, and R. Ott, Thermalization of Gauge Theories from their Entanglement Spectrum, Phys. Rev. Lett. **129**, 011601 (2022).

[108] H. Riechert, J. C. Halimeh, V. Kasper, L. Bretheau, E. Zohar, P. Hauke, and F. Jendrzejewski, Engineering a U(1) lattice gauge theory in classical electric circuits, Phys. Rev. B **105**, 205141 (2022).

[109] J. C. Halimeh, L. Homeier, C. Schweizer, M. Aidelsburger, P. Hauke, and F. Grusdt, Stabilizing lattice gauge theories through simplified local pseudogenerators, Phys. Rev. Res. **4**, 033120 (2022).

[110] J. Zhang, R. Ferguson, S. Kühn, J. F. Haase, C. M. Wilson, K. Jansen, and C. A. Muschik, Simulating gauge theories with variational quantum eigensolvers in superconducting microwave cavities, arXiv:2108.08248.

[111] M. S. Alam, S. Hadfield, H. Lamm, and A. C. Y. Li (SQMS Collaboration), Primitive quantum gates for dihedral gauge theories, Phys. Rev. D **105**, 114501 (2022).

[112] P. Deliyannis, M. Freytsis, B. Nachman, and C. W. Bauer, Practical considerations for the preparation of multivariate Gaussian states on quantum computers, arXiv:2109.10918.

[113] M. A. Perlin, D. Barberena, M. Mamaev, B. Sundar, R. J. Lewis-Swan, and A. M. Rey, Engineering infinite-range SU(n) interactions with spin-orbit-coupled fermions in an optical lattice, Phys. Rev. A **105**, 023326 (2022).

[114] L. Funcke, T. Hartung, K. Jansen, S. Kühn, M. Schneider, P. Stornati, and X. Wang, Towards quantum simulations in particle physics and beyond on noisy intermediate-scale quantum devices, Philos. Trans. A. Math. Phys. Eng. Sci. **380**, 20210062 (2021).

[115] E. Gustafson, B. Holzman, J. Kowalkowski, H. Lamm, A. C. Y. Li, G. Perdue, S. Boixo, S. Isakov, O. Martin, R. Thomson *et al.*, Large scale multi-node simulations of Z_2 gauge theory quantum circuits using Google Cloud Platform, arXiv:2110.07482 [quant-ph].

[116] M. Van Damme, J. Mildenberger, F. Grusdt, P. Hauke, and J. C. Halimeh, Suppressing nonperturbative gauge errors in the thermodynamic limit using local pseudogenerators, arXiv:2110.08041.

[117] A. Kan, L. Funcke, S. Kühn, L. Dellantonio, J. Zhang, J. F. Haase, C. A. Muschik, and K. Jansen, 3+1D θ-term on the lattice from the Hamiltonian perspective, PoS **LATTICE2021**, 112 (2022).

[118] S. Ashkenazi and E. Zohar, Duality as a feasible physical transformation for quantum simulation, Phys. Rev. A **105**, 022431 (2022).

[119] C. Alexandrou, L. Funcke, T. Hartung, K. Jansen, S. Kühn, G. Polykratis, P. Stornati, X. Wang, and T. Weber, Investigating the variance increase of readout error mitigation through classical bit-flip correction on IBM and Rigetti quantum computers, PoS **LATTICE2021**, 243 (2022).

[120] C. W. Bauer and D. M. Grabowska, Efficient representation for simulating U(1) gauge theories on digital quantum computers at all values of the coupling, Phys. Rev. D **107**, L031503 (2023).

[121] X. Wang, X. Feng, L. Funcke, T. Hartung, K. Jansen, S. Kühn, G. Polykratis, and P. Stornati, Model-independent error mitigation in parametric quantum circuits and depolarizing projection of quantum noise, PoS **LATTICE2021**, 603 (2022).

[122] G. Iannelli and K. Jansen, Noisy Bayesian optimization for variational quantum eigensolvers, PoS **LATTICE2021**, 251 (2022).

[123] K. Yeter-Aydeniz, Z. Parks, A. Nair, E. Gustafson, A. F. Kemper, R. C. Pooser, Y. Meurice, and P. Dreher, Measuring NISQ gate-based qubit stability using a 1+1 field theory and cycle benchmarking, arXiv:2201.02899.

[124] T. Hartung, T. Jakobs, K. Jansen, J. Ostmeyer, and C. Urbach, Digitising SU(2) gauge fields and the freezing transition, Eur. Phys. J. C **82**, 237 (2022).

[125] M. Illa and M. J. Savage, Basic elements for simulations of standard model physics with quantum annealers: Multigrid and clock states, Phys. Rev. A **106**, 052605 (2022).

[126] Y. Ji, H. Lamm, and S. Zhu, Gluon digitization via character expansion for quantum computers, arXiv:2203.02330.

[127] M. Carena, H. Lamm, Y.-Y. Li, and W. Liu, Improved Hamiltonians for Quantum Simulations of Gauge Theories, Phys. Rev. Lett. **129**, 051601 (2022).

[128] J. C. Halimeh, L. Barbiero, P. Hauke, F. Grusdt, and A. Bohrdt, Robust quantum many-body scars in lattice gauge theories, arXiv:2203.08828.

[129] J. Mildenberger, W. Mruczkiewicz, J. C. Halimeh, Z. Jiang, and P. Hauke, Probing confinement in a $\mathbb{Z}_2$ lattice gauge theory on a quantum computer, arXiv:2203.08905.

[130] P. Deliyannis, J. Sud, D. Chamaki, Z. Webb-Mack, C. W. Bauer, and B. Nachman, Improving quantum simulation efficiency of final state radiation with dynamic quantum circuits, Phys. Rev. D **106**, 036007 (2022).

[131] A. Ciavarella, N. Klco, and M. J. Savage, Some conceptual aspects of operator design for quantum simulations of non-Abelian lattice gauge theories, arXiv:2203.11988.

[132] S. Caspar and H. Singh, From Asymptotic Freedom to θ Vacua: Qubit Embeddings of the O(3) Nonlinear σ Model, Phys. Rev. Lett. **129**, 022003 (2022).

[133] C. W. Bauer, Z. Davoudi, A. B. Balantekin, T. Bhattacharya, M. Carena, W. A. de Jong, P. Draper, A. El-Khadra, N. Gemelke, M. Hanada, D. Kharzeev, H. Lamm, Y.-Y. Li, J. Liu, M. Lukin, Y. Meurice, C. Monroe, B. Nachman, G. Pagano, J. Preskill *et al.*, Quantum simulation for high energy physics, arXiv:2204.03381.

[134] J. C. Halimeh, I. P. McCulloch, B. Yang, and P. Hauke, Tuning the topological θ-angle in cold-atom quantum simulators of gauge theories, PRX Quantum **3**, 040316 (2022).
[135] J. C. Halimeh and P. Hauke, Stabilizing gauge theories in quantum simulators: A brief review, arXiv:2204.13709.
[136] I. Raychowdhury, Z. Davoudi, and A. Shaw, Exploring different formulations of non-Abelian lattice gauge theories for Hamiltonian simulation, PoS **LATTICE2021**, 277 (2022).
[137] P. Dreher, E. Gustafson, Y. Zhu, N. M. Linke, and Y. Meurice, Real-time quantum calculations of phase shifts on NISQ hardware platforms using wavepacket time delay, PoS **LATTICE2021**, 464 (2022).
[138] T. Greenberg, G. Pardo, A. Fortinsky, and E. Zohar, Resource-efficient quantum simulation of lattice gauge theories in arbitrary dimensions: Solving for Gauss' law and fermion elimination, arXiv:2206.00685.
[139] C. Tüysüz, G. Clemente, A. Crippa, T. Hartung, S. Kühn, and K. Jansen, Classical splitting of parametrized quantum circuits, arXiv:2206.09641.
[140] J. Bringewatt and Z. Davoudi, Parallelization techniques for quantum simulation of fermionic systems, arXiv:2207.12470.
[141] D. M. Grabowska, C. Kane, B. Nachman, and C. W. Bauer, Overcoming exponential scaling with system size in Trotter-Suzuki implementations of constrained Hamiltonians: 2+1 U(1) lattice gauge theories, arXiv:2208.03333.
[142] M. Asaduzzaman, G. C. Toga, S. Catterall, Y. Meurice, and R. Sakai, Quantum simulation of the N-flavor Gross-Neveu model, Phys. Rev. D **106**, 114515 (2022).
[143] M. Carena, E. J. Gustafson, H. Lamm, Y.-Y. Li, and W. Liu, Gauge theory couplings on anisotropic lattices, Phys. Rev. D **106**, 114504 (2022).
[144] E. J. Gustafson, H. Lamm, F. Lovelace, and D. Musk, Primitive quantum gates for an SU(2) discrete subgroup: BT, Phys. Rev. D **106**, 114501 (2022).
[145] Z. Davoudi, N. Mueller, and C. Powers, Toward quantum computing phase diagrams of gauge theories with thermal pure quantum states, arXiv:2208.13112.
[146] A. Avkhadiev, P. E. Shanahan, and R. D. Young, Strategies for quantum-optimized construction of interpolating operators in classical simulations of lattice quantum field theories, Phys. Rev. D **107**, 054507 (2023).
[147] W. Jang, K. Terashi, M. Saito, C. W. Bauer, B. Nachman, Y. Iiyama, R. Okubo, and R. Sawada, Initial-state dependent optimization of controlled gate operations with quantum computer, Quantum **6**, 798 (2022).
[148] G. Clemente, A. Crippa, and K. Jansen, Strategies for the determination of the running coupling of $(2+1)$-dimensional qed with quantum computing, Phys. Rev. D **106**, 114511 (2022).
[149] H. Singh, Qubit regularized $O(N)$ nonlinear sigma models, Phys. Rev. D **105**, 114509 (2022).
[150] J. Y. Araz, S. Schenk, and M. Spannowsky, Toward a quantum simulation of nonlinear sigma models with a topological term, Phys. Rev. A **107**, 032619 (2023).
[151] T. Bhattacharya, A. J. Buser, S. Chandrasekharan, R. Gupta, and H. Singh, Qubit Regularization of Asymptotic Freedom, Phys. Rev. Lett. **126**, 172001 (2021).
[152] S. Chandrasekharan, B. Scarlet, and U.-J. Wiese, From spin ladders to the 2D O(3) model at non-zero density, Comput. Phys. Commun. **147**, 388 (2002).
[153] R. Brower, S. Chandrasekharan, S. Riederer, and U. Wiese, D theory: Field quantization by dimensional reduction of discrete variables, Nucl. Phys. B **693**, 149 (2004).
[154] A. Alexandru, P. F. Bedaque, A. Carosso, M. J. Cervia, and A. Sheng, Qubitization strategies for bosonic field theories, Phys. Rev. D **107**, 034503 (2023).
[155] F. Bruckmann, K. Jansen, and S. Kühn, O(3) nonlinear sigma model in $1+1$ dimensions with matrix product states, Phys. Rev. D **99**, 074501 (2019).
[156] S. Chakravarty, B. I. Halperin, and D. R. Nelson, Two-dimensional quantum Heisenberg antiferromagnet at low temperatures, Phys. Rev. B **39**, 2344 (1989).
[157] B. B. Beard, M. Pepe, S. Riederer, and U. J. Wiese, Efficient cluster algorithm for CP(N-1) models, Comput. Phys. Commun. **175**, 629 (2006).
[158] S. R. Beane, W. Detmold, K. Orginos, and M. J. Savage, Uncertainty quantification in lattice QCD calculations for nuclear physics, J. Phys. G: Nucl. Part. Phys. **42**, 034022 (2015).
[159] S. Caracciolo, R. G. Edwards, A. Pelissetto, and A. D. Sokal, Asymptotic scaling in the two-dimensional O(3) σ model at correlation length 10^5, Phys. Rev. Lett. **75**, 1891 (1995).
[160] M. Fishman, S. R. White, and E. M. Stoudenmire, Codebase release 0.3 for ITensor, SciPost Phys. Codebases, 4 (2022).
[161] M. Fishman, S. R. White, and E. M. Stoudenmire, The ITensor Software Library for tensor network calculations, SciPost Phys. Codebases, 4 (2022).
[162] S. R. White, Density Matrix Formulation for Quantum Renormalization groups, Phys. Rev. Lett. **69**, 2863 (1992).
[163] S. R. White, Density-matrix algorithms for quantum renormalization groups, Phys. Rev. B **48**, 10345 (1993).
[164] F. Verstraete, J. J. García-Ripoll, and J. I. Cirac, Matrix Product Density Operators: Simulation of Finite-Temperature and Dissipative Systems, Phys. Rev. Lett. **93**, 207204 (2004).
[165] G. Semeghini, H. Levine, A. Keesling, S. Ebadi, T. T. Wang, D. Bluvstein, R. Verresen, H. Pichler, M. Kalinowski, R. Samajdar, A. Omran, S. Sachdev, A. Vishwanath, M. Greiner, V. Vuletić, and M. D. Lukin, Probing topological spin liquids on a programmable quantum simulator, Science **374**, 1242 (2021).
[166] H. Bernien, S. Schwartz, A. Keesling, H. Levine, A. Omran, H. Pichler, S. Choi, A. S. Zibrov, M. Endres, M. Greiner *et al.*, Probing many-body dynamics on a 51-atom quantum simulator, Nature (London) **551**, 579 (2017).
[167] A. N. Ciavarella, S. Caspar, H. Singh, M. J. Savage, and P. Lougovski, Floquet engineering Heisenberg from Ising using constant drive fields for quantum simulation, arXiv:2207.09438.
[168] A. N. Ciavarella, S. Caspar, M. Illa, and M. J. Savage, State preparation in the Heisenberg model through adiabatic spiraling, arXiv:2210.04965.
[169] J. Haegeman, J. I. Cirac, T. J. Osborne, I. Pižorn, H. Verschelde, and F. Verstraete, Time-Dependent Variational Principle for Quantum Lattices, Phys. Rev. Lett. **107**, 070601 (2011).
[170] J. Haegeman, C. Lubich, I. Oseledets, B. Vandereycken, and F. Verstraete, Unifying time evolution and optimization with matrix product states, Phys. Rev. B **94**, 165116 (2016).
[171] M. Yang and S. R. White, Time-dependent variational principle with ancillary Krylov subspace, Phys. Rev. B **102**, 094315 (2020).

[172] A. Omran, H. Levine, A. Keesling, G. Semeghini, T. T. Wang, S. Ebadi, H. Bernien, A. S. Zibrov, H. Pichler, S. Choi, J. Cui, M. Rossignolo, P. Rembold, S. Montangero, T. Calarco, M. Endres, M. Greiner, V. Vuletić, and M. D. Lukin, Generation and manipulation of Schrödinger cat states in Rydberg atom arrays, Science **365**, 570 (2019).

[173] T. Graham, Y. Song, J. Scott, C. Poole, L. Phuttitarn, K. Jooya, P. Eichler, X. Jiang, A. Marra, B. Grinkemeyer *et al.*, Demonstration of multi-qubit entanglement and algorithms on a programmable neutral atom quantum computer, Nature (London) **604**, 457 (2022).

[174] P. Huft, Y. Song, T. M. Graham, K. Jooya, S. Deshpande, C. Fang, M. Kats, and M. Saffman, Simple, passive design for large optical trap arrays for single atoms, Phys. Rev. A **105**, 063111 (2022).

[175] R. D. Peccei and H. R. Quinn, CP Conservation in the Presence of Pseudoparticles, Phys. Rev. Lett. **38**, 1440 (1977).

[176] F. Wilczek, Problem of Strong p and t Invariance in the Presence of Instantons, Phys. Rev. Lett. **40**, 279 (1978).

[177] N. Mueller, J. A. Carolan, A. Connelly, Z. Davoudi, E. F. Dumitrescu, and K. Yeter-Aydeniz, Quantum computation of dynamical quantum phase transitions and entanglement tomography in a lattice gauge theory, arXiv:2210.03089.

[178] https://itconnect.uw.edu/research/hpc.

[179] https://phys.washington.edu.

[180] https://www.artsci.washington.edu.